ALEPH 99-038
CONF 99-022
May 21, 1999

PRELIMINARY
A Study of the Photon Structure Function $\mathrm{F}_2^\gamma(x, Q^2)$ using Two-Dimensional Unfolding

The ALEPH Collaboration

Abstract

Data taken with the ALEPH detector at LEP II have been used to measure the photon structure function F_2^γ. The data were collected in 1997 at a centre-of-mass energy of $\sqrt{\mathrm{s}} \approx 183$ GeV and analysed in the two Q^2 ranges from 7 to 24 and from 17 to 200 GeV^2. To determine F_2^γ, a two-dimensional unfolding method employing the principle of maximum entropy is used, which reduces the errors compared to one-dimensional methods. The results are compared to the predictions of several theoretical models.

Contribution to PHOTON99 Conference, Freiburg, May 1999

Contacts: Klaus.Affholderbach@cern.ch, Glen.Cowan@cern.ch

1 Introduction

A measurement of the photon structure function F_2^γ based on data from the ALEPH experiment at the LEP II e^+e^- collider is presented. In e^+e^- collisions, each of the incoming beam leptons acts as a source of virtual photons. Events where one beam lepton is scattered at a sufficiently large angle to be detected are said to be 'single-tagged'. These events can be interpreted as the deep inelastic scattering of an electron by an almost real photon, and thus used to determine F_2^γ. Single-tag events with hadronic final states were selected from the data recorded by the ALEPH detector in 1997 at a centre-of-mass energy of $\sqrt{s} = 183$ GeV. The event sample corresponded to an integrated luminosity of 53 pb^{-1}.

The measured momenta of the tagged lepton and particles in the hadronic final state can be used to measure the following quantities,

$$Q^2 \;=\; 2E_{\mathrm{tag}}E_{\mathrm{beam}}(1-\cos\Theta_{\mathrm{tag}})\;, \tag{1}$$

$$x \;=\; \frac{Q^2}{2q\cdot p} \;\approx\; \frac{Q^2}{Q^2+W^2}\;, \tag{2}$$

where $Q^2 = -q^2$ is the negative four-momentum squared of the virtual photon emitted from the tagged electron, and E_{tag} and Θ_{tag} are the measured energy and the polar angle of the tagged lepton. The Bjorken variable x corresponds to the fraction of the target photon momentum carried by the struck quark (in the Breit frame), W is the invariant mass of the $\gamma\gamma$ system, and p and q are the four-momenta of the two virtual photons.

The cross-section for deep inelastic electron-photon scattering can be expressed as [1]

$$\frac{d^2\sigma_{\mathrm{e}\gamma\to\mathrm{e}X}}{dxdQ^2} \;=\; \frac{2\pi\alpha_{\mathrm{em}}^2}{xQ^4}\left[\left(1+(1-y)^2\right)F_2^\gamma(x,Q^2) - y^2F_L^\gamma(x,Q^2)\right] \tag{3}$$

where y is the inelasticity of the event,

$$y = \frac{q\cdot p}{kp} \;\approx\; 1-\frac{E_{\mathrm{tag}}}{E_{\mathrm{beam}}}\cos^2\left(\frac{\Theta_{\mathrm{tag}}}{2}\right)\;, \tag{4}$$

and k represents the four-momentum of the incident lepton which scatters with high momentum transfer Q^2. In the kinematic region studied, the contribution of the term proportional to $F_L^\gamma(x,Q^2)$ is negligible since $y \ll 1$ holds. Equation (3) can thus be used to relate the distribution of x and Q^2 to the structure function F_2^γ. In this analysis, F_2^γ is measured in two ranges of Q^2 having mean values of 13.7 and 56.5 GeV^2.

In order to measure the cross section $d^2\sigma/dxdQ^2$, corrections must be applied to account for the incomplete acceptance and resolution of the detector. The correction procedure (unfolding) makes use of distributions from Monte Carlo models, and the uncertainty from model dependence has been a major source of systematic error in previous measurements.

For this analysis a two-dimensional unfolding method has been developed which results in smaller systematic and statistical errors.

2 Experimental method

The ALEPH detector and its performance have been described in detail elsewhere [2, 3]. Charged tracks and neutral calorimeter energy as defined by the ALEPH energy flow package [4] are used in this analysis.

The following selection criteria were applied in order to obtain a sample of single-tag two-photon events. The event must contain a tagged electron or positron. A tag is defined as a cluster in one of the small angle luminosity calorimeters SICAL or LCAL. The energy and angle of the tag are required to be $E_{\rm tag} > 60$ GeV and $35 \leq \Theta_{\rm tag} \leq 54$ mrad in case of a SICAL tagged event and $E_{\rm tag} > 50$ GeV and $60 \leq \Theta_{\rm tag} \leq 155$ mrad for LCAL tagged events. To ensure that the event is single- and not double-tagged, there must be no cluster with $E_{\rm tag} > 20$ GeV in one of the small angle luminosity calorimeters opposite to the tag direction. The visible hadronic final state has to consist of at least three charged tracks and has to have an invariant mass $W_{\rm vis}$ greater than 2 GeV. Furthermore, the event must contain a reconstructed vertex within 5 cm in the z direction and 1 cm in the radial direction from the nominal interaction point. To eliminate events originating from lepton production, an identified electron or muon with $|\cos\Theta| < 0.8$ and $E > 2$ GeV must not be observed. After applying these cuts, the data were split into two samples according to their Q^2 values.

The only relevant residual background remaining in the final sample originates from the process $\gamma\gamma \to \tau^+\tau^-$. The contamination of the final sample with those events has been determined using Monte Carlo simulations. The expected fractions are 2.3% and 4.5% for SICAL and LCAL tagged events, respectively. These background events are uniformaly distributed in x and have been subtracted. In the lower Q^2 range from 7 to 24 GeV^2, 1208 events remain while the sample in the range from 17 to 200 GeV^2 contains 861 events.

3 Unfolding

An unfolding procedure employing the principle of maximum entropy (MaxEnt) is used to correct the distributions for finite resolution and acceptance. As this aspect of the analysis is new, it will be described in some detail here. More information can be found in [5, 6].

The need for these corrections can be seen from Fig. 1. This shows scatter plots of true and measured ('visible') values of the variables x and Q^2 obtained from events generated with HERWIG [7] and SaS [8] parametrization for F_2^γ and passed through a full detector simulation. As can be seen from the scatter plot for x, the measured and true values are often significantly different, which leads to a considerable smearing of the x distribution.

The resolution in Q^2, however, is quite good, and thus the problem of unfolding is mainly one of constructing estimators for the x distribution. Once $d^2\sigma/dxdQ^2$ has been obtained, it is combined with information on the photon flux to extract F_2^γ (see section 5).

The unfolding of the x distribution is done separately for the two Q^2 regions considered. The parameters to be estimated are the cross sections $d^2\sigma/dxdQ^2$ averaged over each of the M bins, which here are represented by a vector $\vec{\mu} = (\mu_1, \ldots, \mu_M)$. From the selected events one obtains a histogram $\vec{n} = (n_1, \ldots, n_N)$, which is distorted with respect to $\vec{\mu}$ both because of statistical fluctuations as well as from the effects of acceptance and resolution.

The number of entries n_i observed in a given bin i can be treated as a Poisson variable with expectation value $\nu_i = E[n_i]$. The vectors $\vec{\mu}$ and $\vec{\nu}$ are related by

$$\vec{\nu} = R\vec{\mu} + \vec{\beta}\,, \tag{5}$$

where the response matrix R_{ij} represents the probability for an event to be observed in bin i given that its true x value was in bin j, and the vector $\vec{\beta} = (\beta_1, \ldots, \beta_N)$ gives the expected background. The log-likelihood function is

$$\log L(\vec{\mu}) = \sum_{i=1}^{N} \log(n_i \log \nu_i - \nu_i)\,, \tag{6}$$

which is a function of $\vec{\mu}$ because of equation (5).

Because of the large smearing of the x values, the maximum likelihood estimators $\hat{\vec{\mu}} = R^{-1}(\vec{n} - \vec{\beta})$ have very large variances and in fact oscillate wildly from bin to bin. (Here estimators will be denoted by hats.) The variances can be drastically reduced at the price of introducing a small bias by maximizing a combination of $\log L$ and an appropriately chosen regularization function $S(\vec{\mu})$,

$$\varphi(\vec{\mu}, \lambda) = \alpha \log L(\vec{\mu}) + S(\vec{\mu}) + \lambda \left[n_{\rm tot} - \sum_{i=1}^{N} \nu_i \right]\,, \tag{7}$$

with respect to the parameters $\vec{\mu}$ and the Lagrange multiplier λ. The final term in φ restricts the solution to satisfy $\sum_i \nu_i = \sum_{i,j} R_{ij}\mu_j = n_{\rm tot}$, where $n_{\rm tot}$ is the total number of events observed.

The regularization function $S(\vec{\mu})$ is a measure of the smoothness of the unfolded distribution, and thus the regularization parameter α determines the trade-off between likelihood and smoothness. The regularization function used in the analysis here is the Shannon entropy [9],

$$S(\vec{\mu}) = -\sum_{j=1}^{M} \frac{\mu_j}{\mu_{\rm tot}} \log\left(\frac{\mu_j}{\mu_{tot}}\right)\,, \tag{8}$$

with $\mu_{tot} = \sum_{j=1}^{M} \mu_j$. The entropy-based regularization function makes no reference to the relative locations of any of the bins, which has the advantage that the bins at the edges

of the distribution are treated on the same footing as those in the middle. In addition, use of MaxEnt, i.e. equation (8), can be directly applied to multidimensional distributions, which will be discussed below. The regularization parameter α is fixed by first constructing estimators for the biases $b_i = E[\hat{\mu}_i] - \mu_i$ (i.e. expectation value minus true value), and then requiring that these be consistent with zero to within their own statistical errors (cf. [6]).

An important source of systematic uncertainty in previous measurements of F_2^γ has been related to the model dependence of the response matrix R. To determine R, a Monte Carlo model must be used to generate events which are then processed by the detector simulation program. The x distribution of the generator is itself not a significant source of model dependence, since the response matrix element R_{ij} represents the conditional probability for an event to be observed in bin i given that it was created in bin j. By construction this is independent of the rate with which events are produced in bin j, i.e. it is independent of the model's x distribution.

The true value of x, however, is not the only variable that has an influence on the probability to measure a given value x'. For example, if the hadrons are mostly at low angles with respect to the beam line, then the resolution for x will be poor. This occurs because at low angles the particles will either be lost or will enter detector elements such as the luminosity monitors, which are not optimized for measuring hadronic energy. Since different models have in general different distributions for all of the variables that characterize the final state hadrons, each will lead to somewhat different response matrices R, and hence to different results for the unfolded x distribution.

A method to reduce this model dependence is to measure for each event not only x but in addition some other variable characterizing the final state. For this we have used the variable E_{17}, defined as the total energy of the particles having angles with respect to the beam line less than 17°. Monte Carlo studies show that the x resolution degrades considerably for increasing E_{17}. The two-dimensional distribution is unfolded using the procedure outlined above, and the result is then integrated over E_{17} yielding the unfolded x distribution.

In addition to reducing the model dependence, two-dimensional unfolding leads to smaller statistical errors. This is because in the one-dimensional case, the effective weight of each event is determined by the average x resolution in the bin. With two-dimensional unfolding, those events with low E_{17} are given a higher weight in the final result, since for them x is determined more accurately. Thus the events with poor x resolution do not dilute the information carried by those for which x is better measured. The resolution of x in four different bins of E_{17} is shown in Fig. 2. The improvements achievable by two-dimensional unfolding were investigated quantitatively in [5].

4 Monte Carlo models

The unfolding procedure described above seeks to reduce the dependence on Monte Carlo models. Nevertheless, model dependence remains a significant source of systematic

uncertainty, and the event generators used should therefore be as accurate as possible.

In this analysis the model HERWIG 5.9 [7] has been used with two different structure function parametrizations as input: that of Glück, Reya and Vogt (GRV)[10] and Set 1D of Schuler and Sjöstrand (SaS)[8]. All other parameters of the program were set to their default values apart from the intrinsic transverse momentum k_t of the partons in the target photon (see [5]). In addition, the PHOJET[11] program was used.

Distributions of several kinematic variables are shown in Fig. 3, where the SICAL-tagged data are compared to the model predictions mentioned above. Comparisons of LCAL-tagged data with predictions are shown in Fig. 4. As can be seen from the plots, PHOJET is in poor agreement with the data for the higher Q^2 range (LCAL tag), and therefore it is not used there to determine the response matrix.

5 Results for F_2^γ

The unfolding method described in section 3 was used to obtain the x distributions dN/dx in the two Q^2 ranges. The response matrices have been calculated from the models mentioned in section 4. F_2^γ was extracted using

$$\hat{F}_2^\gamma(x, \langle Q^2 \rangle)_{\text{meas.}} = \frac{\left(\frac{dN}{dx}\right)_{\text{meas.}}}{\left(\frac{dN}{dx}\right)_{\text{ref.}}} \cdot F_2^\gamma(x, \langle Q^2 \rangle)_{\text{ref.}}, \tag{9}$$

where *ref.* denotes the parametrisation for F_2^γ used in the model to obtain the response matrix. The final distributions were obtained by averaging the results using the different models.

The systematic errors due to model dependence were calculated from the spread of the results based on the different models. A systematic uncertainty due to the choice of the regularization parameter α was estimated by setting it to give a much stronger level of smoothing; the changes in the results are in all cases much smaller than the model uncertainty.

In addition, systematic uncertainties which could result from possible imperfections of the detector simulation were investigated. For this purpose the analysis was repeated with energy scales of various subdetectors shifted by amounts conservatively corresponding to their systematic uncertainties. The shifts in the final results were small compared to those stemming from the model dependence of the response matrices.

The final results for F_2^γ are shown in Fig. 5. The inner error bars are statistical errors only, the total error bars represent the quadratic sum of statistical and systematic errors. The bin-to-bin correlations between adjacent bins lie in the range of -0.7 to -0.28 and are thus similar to those obtained with other unfolding methods. The measurements are compared to the predictions of the HERWIG model using the GRV and

SaS parametrizations for F_2^γ mentioned above as well as that of Abramowicz, Charchula and Levy (LAC 1) [12]. In both Q^2 ranges, all of the parametrizations provide a good description of the data for $x > 0.1$. For lower x, GRV is found to give the best description. As has been seen previously (see e.g. [13]), the LAC values are significantly too high at low x. In addition, there is evidence that the SaS prediction is too low at low x.

$\langle Q^2 \rangle = 13.7\,\mathrm{GeV}^2$ (this analysis)				$\langle Q^2 \rangle = 9.9\,\mathrm{GeV}^2$ (from [13])			
x-range	F_2^γ/α	Stat. Error	Syst. Error	x-range	F_2^γ/α	Stat. Error	Syst. Error
0.003 - 0.023	0.28	5.3 %	6.3 %				
				0.005 - 0.08	0.30	6.6 %	6.6 %
0.023 - 0.092	0.34	7.5 %	5.3 %				
0.092 - 0.213	0.34	10.8 %	8.0 %	0.08 - 0.20	0.40	7.5 %	17.5 %
0.213 - 0.386	0.35	13.6 %	15.7 %	0.20 - 0.40	0.41	12.2 %	22.0 %
0.386 - 0.786	0.43	11.1 %	10.5 %	0.40 - 0.80	0.27	48.1 %	33.3 %

Table 1: Comparison of F_2^γ derived from the SICAL-tagged data to a previously published measurement in a similar Q^2 range.

In Table 1 the results and errors for the SICAL-tagged data are compared to a previously published measurement of F_2^γ based on a one-dimensional unfolding method in a similar Q^2 range [13]. both measurements use aproximately the same number of observed events. The statistical errors in both measurements are in general of the same order, while the systematic uncertainties in this analysis are found to be significantly reduced.

6 Conclusions

Single-tagged two photon events recorded by the ALEPH detector at LEP II have been studied. Distributions of kinematic variables were compared to predictions of Monte Carlo models including effects of the detector. For the Q^2 range from 7 to 24 GeV^2, discrepancies between the data and the PHOJET prediction are only moderate, but for $17 < Q^2 < 200$ GeV^2, large differences are seen. The GRV and SaS parametrizations used with the HERWIG model give qualitatively good descriptions of the data for both Q^2 ranges.

A two-dimensional unfolding technique using the principle of maximum entropy has been used to measure the photon structure function F_2^γ. This unfolding method leads to smaller statistical errors and a reduced model dependence compared to one-dimensional procedures. The results have been compared to predictions of different models and are

found to be well described by the GRV parametrization of F_2^γ used with the HERWIG model. At low x, the data are found to be higher than the SaS parametrization, and considerably lower than that of LAC .

Acknowledgements

We wish to thank our colleagues from the accelerator division for the successful operation of the LEP machine, and the engineers and technical staff in all our institutes for their contribution to the good performance of ALEPH. Those of us from non–member states thank CERN for its hospitality.

References

[1] C. Berger and W. Wagner, *Phys. Rep.* **146** (1987) 1.

[2] ALEPH Collab., D. Decamp et al., *Nucl. Instr. Meth.* **A294** (1990) 121.

[3] ALEPH Collab., D. Buskulic et al., *Nucl. Instr. Meth.* **A360** (1995) 481.

[4] ALEPH Collab., D. Decamp et al., *Phys. Lett.* **B246** (1990) 306.

[5] S. Cartwright et al., *J. Phys.* **G24** (1998) 457.

[6] Glen Cowan, *Statistical Data Analysis*, Clarendon Press, Oxford ,1998.

[7] G. Marchesini et al., *Comp. Phys. Comm.* **67** (1992) 465.

[8] G.A. Schuler and T. Sjöstrand, *Z. Phys.* **C68** (1995) 607.

[9] C.E.Shannon, *Bell Sys. Tech.* **J.27** (1948) 379.

[10] M. Glück, E. Reya and A. Vogt, *Phys. Rev.* **D45** (1992) 3986;
M. Glück, E. Reya and A. Vogt, *Phys. Rev.* **D46** (1992) 1974.

[11] R. Engel, *Z. Phys.* **C66** (1995) 203;
R. Engel and J. Ranft, *Phys. Rev.* **D54** (1996) 4244.

[12] H. Abramowicz, K. Charchula and A. Levy, Phys. Lett. **269B** (1991) 458.

[13] ALEPH Collab., R. Barate et al., *Measurement of the hadronic photon structure function at LEP I for Q^2 values between 9.9 and 284 GeV^2*, CERN EP/99-063 (1999), submitted to Physics Letters B.

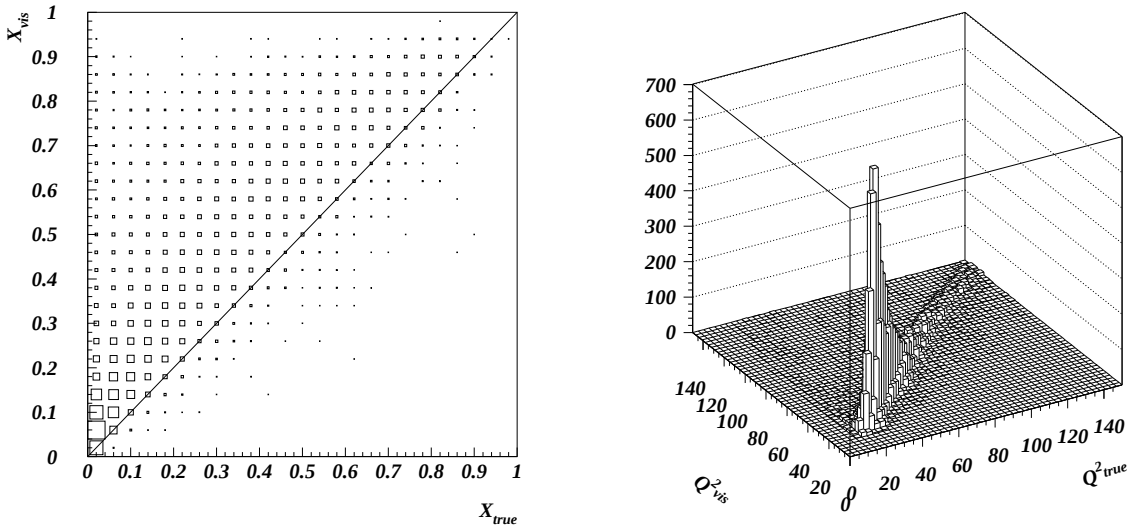

Figure 1: The relationship between reconstructed and true values for x and Q^2 obtained from events simulated using the HERWIG generator and full detector simulation.

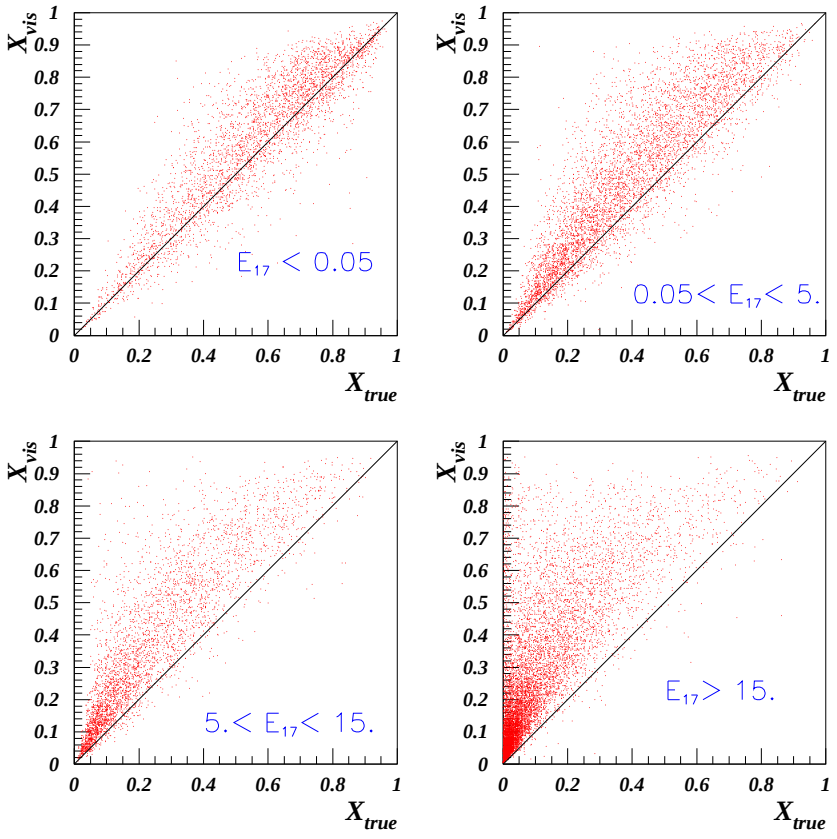

Figure 2: The relationship between reconstructed and true values for x in four subsequent bins of the variable E_{17} obtained from events simulated using the HERWIG generator and full detector simulation.

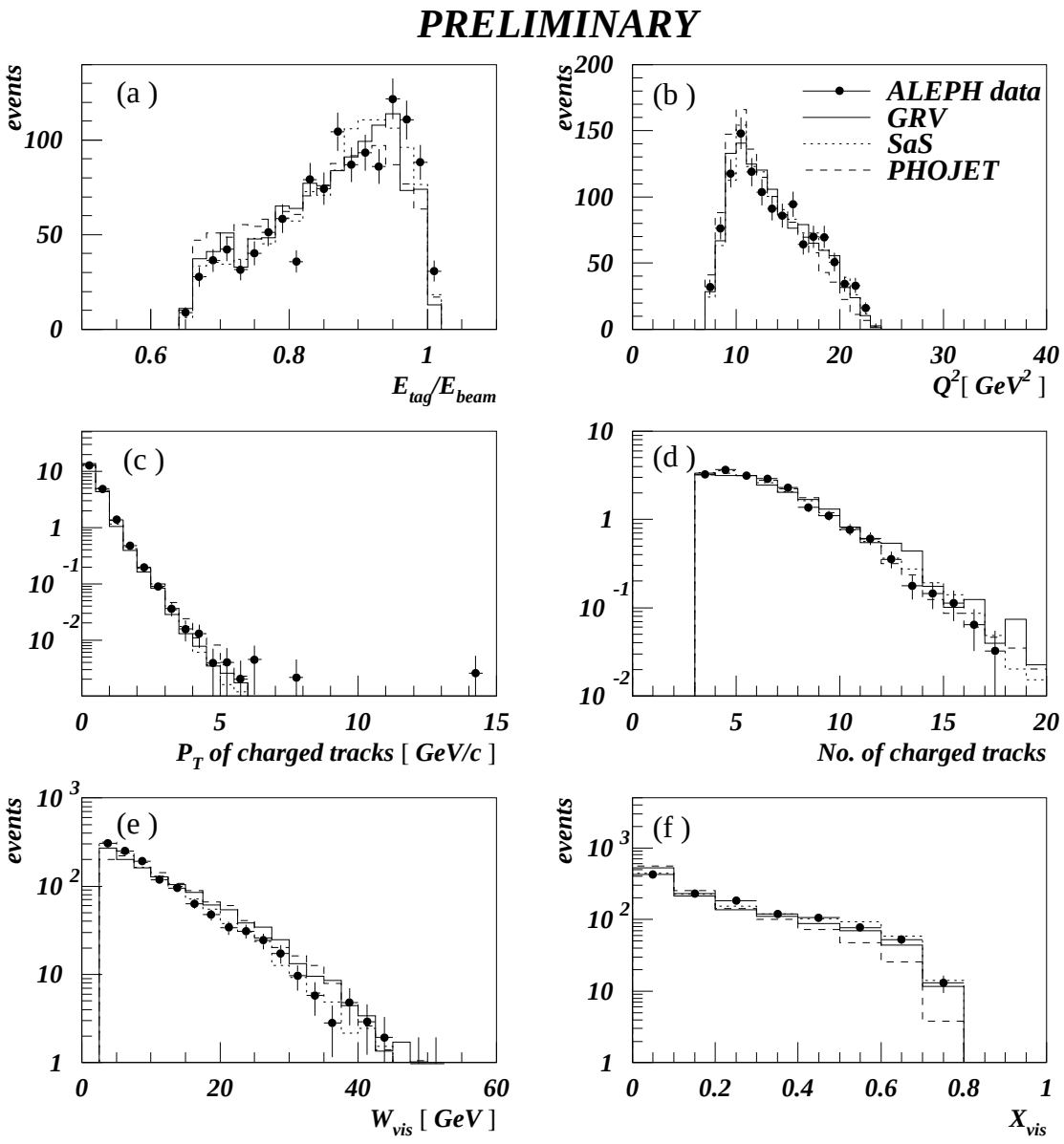

Figure 3: Comparison of data and simulations for SICAL tagged data. Plot (a) shows the ratio of the energy of the tag electron over the beam energy, (b) the Q^2 of the tag, (c) the transverse momentum w.r.t the beam direction, (d) the number of tracks from charged particles in the final state. Plot (e) and (f) show the $W_{\rm vis}$ and $x_{\rm vis}$ distributions.

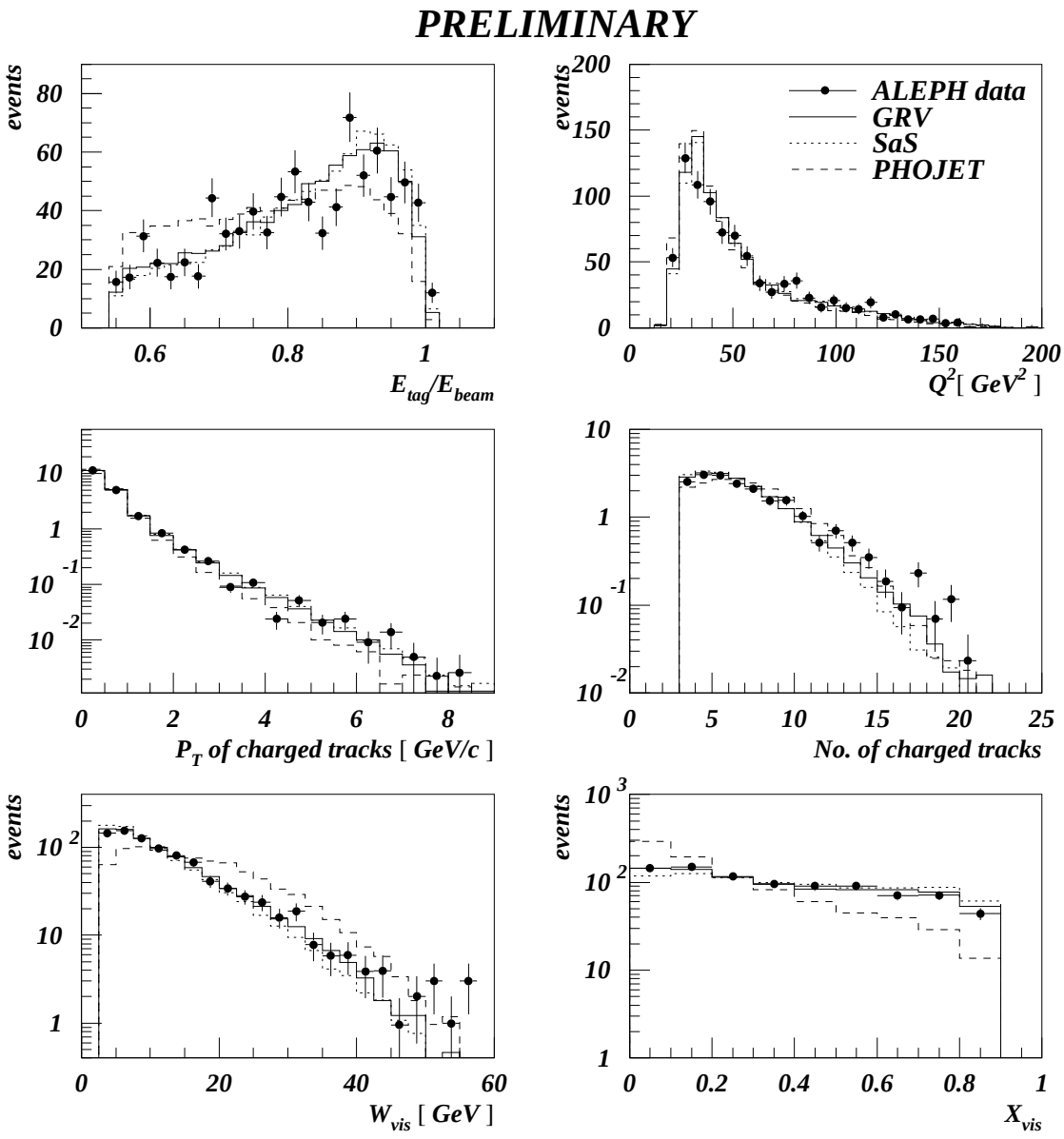

Figure 4: The same as Fig. 3, but for LCAL tagged data.

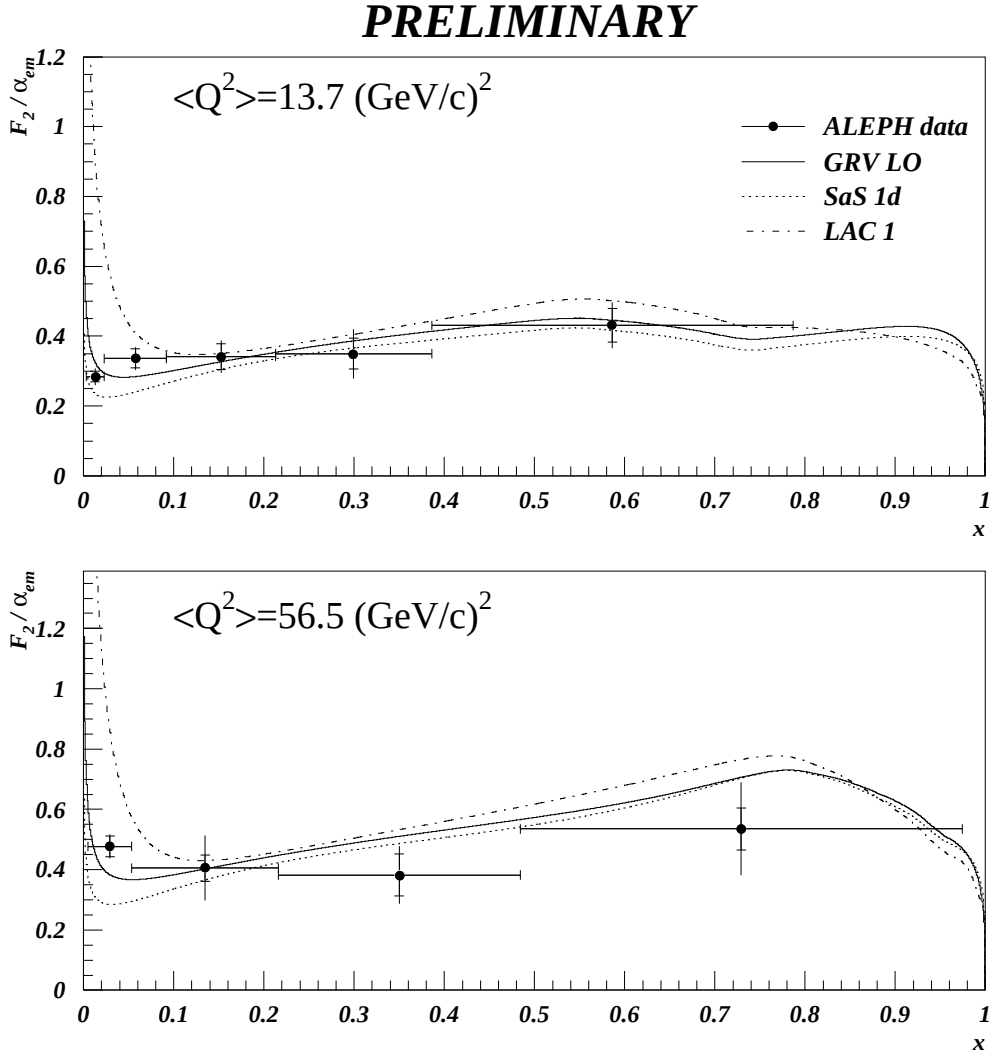

Figure 5: Results for the measurement of F_2^γ as a function of x in two bins of Q^2. The *points* show the measured F_2^γ. The inner error bars represent the statistical errors only, while the total error bars are the quadratic sum of statistical and systematic errors. The *solid* line denotes F_2^γ derived from the GRV parametrization, the *dotted* line denotes the F_2^γ derived from the SaS1d parametrization and the *dashed-dotted* one shows F_2^γ obtained with the parametrization from LAC.